A brief introduction to low-power electrical energy harvesting mechanisms and configurations

Breve introducción a los mecanismos y configuraciones de cosechadores de energía eléctrica de baja potencia

K. Morales-Almanza [ID] [a], G. Lara-Hernández [ID] [a], J. P Rodríguez-Jarquin [ID] [a], X. Xu [ID] [b], J. J. A. Flores-Cuautle [ID] [c*]

[a] *TecNM-IT Orizaba Oriente 9, 94320 Orizaba, México.*
[b] *Lab of Modern Acoustics, Institute of Acoustics, Nanjing University, Nanjing 210093, China.*
[c] *CONACYT/ TecNM-IT Orizaba Oriente 9, 94320 Orizaba, México.*

Abstract

Technological development and a more environmentally friendly culture have encouraged alternative energy generation methods. Exploring all possible forms of production power has risen in several fields. Consequently, electronic devices leave out their conventional power supplies, meeting their energy needs without affecting the environment. This text overviews low-power applications' energy harvesting mechanisms, devices, and power generation capabilities. The piezoelectric, triboelectric, thermoelectric, and electromagnetic fundamental physics for energy harvesting applications is introduced. Examples of applications of energy harvesting systems are also presented. A summary of the power generation process is given, followed by a description of each physical mechanism used to harvest energy.

Keywords: Harvester, piezoelectric, triboelectric, electromagnetic, thermoelectric.

Resumen

El desarrollo tecnológico y una cultura más respetuosa con el medio ambiente han fomentado métodos alternativos de generación de energía. La exploración de todas las formas posibles de producción de energía ha aumentado en varios campos. En consecuencia, los dispositivos electrónicos dejan de lado sus fuentes de alimentación convencionales, satisfaciendo sus necesidades energéticas sin afectar al medio ambiente. Este texto repasa los mecanismos, dispositivos y capacidades de generación de energía de las aplicaciones de baja potencia. Se introduce la física fundamental piezoeléctrica, triboeléctrica, termoeléctrica y electromagnética de las aplicaciones de captación de energía. También se presentan ejemplos de aplicaciones de sistemas de captación de energía. Se ofrece un resumen del proceso de generación de energía, seguido de una descripción de cada mecanismo físico utilizado para cosechar energía.

Palabras Clave: Cosechador, piezoeléctrico, triboeléctrico, electromagnético, termoeléctrico.

1. Introduction

The rise of portable electronic devices and wireless sensing has increased battery improvement research; these low-power electronics use conventional batteries as a primary power source, although there are applications where battery replacement becomes difficult and expensive. Therefore, there is a real need for backup or sustainable energy systems that substitute batteries in those applications.

On the other hand, energy captured from the environment is sustainable energy. Energy capture is mainly based on transforming a physical phenomenon into electrical energy using an appropriate transducer. The generation of electrical energy from converting environmental energy is called energy harvesting. The harvested energy is the preferred option for those low-power systems where battery replacement is unfeasible (Al-Nabulsi et al., 2019; Dagdeviren et al., 2017; Sodano et al., 2004). A search performed on scientific databases (Jonathan Adams, 2019; Thelwall, 2018) over the last ten years reveals 6400 papers related to energy harvesting, and 4200 out of the total were published in the previous five years, as seen in Figure 1. The research fields related to publications are engineering, materials, chemical, and physical sciences, as shown in Figure 1.

Figure 1: Energy harvesting publications and research field in the last ten and five years.

Natural language analysis is presented in Figure 2; this analysis was made by searching the dimensions' database (Jonathan Adams, 2019) using VOSviewer software (van Eck & Waltman, 2010). According to the analysis, three main clusters are related to energy harvesting: materials, physics, and simulations. Therefore, this work is focused on physical mechanisms and materials devoted to harvest energy. Among the available phenomena and mechanisms for energy harvesting, piezoelectric, triboelectric, and thermoelectric–based generators are the main research pathways. Therefore, as mentioned earlier, this paper focuses on the physics of energy harvesting mechanisms. Diverse mechanical configurations and energy harvesting applications are introduced as an example of applications. The preferred energy harvesting sources are wind, sea waves, vibrating sources, and human movement (Lund et al., 2020; Naifar et al., 2020; Y. Wang, Wu, et al., 2020; Y. Wang, Yang, et al., 2020), and corresponding advantages and disadvantages are presented. This work comprehensively overviews different physical mechanisms and devices used to harvest energy.

Figure 2: Keywords influence, and relationships derived from a search over dimensions database (Jonathan Adams, 2019).

1. Background

1.1. Piezoelectrics

The piezoelectric phenomenon is defined as the electrical charge generated by certain materials due to mechanical stress; electrical charge is caused by the material electrical dipole rearrangement resulting from mechanical stress (Jaffe, 1958).

Figure 3 shows the electrical charge generation under tension and compression stress conditions.

Figure 3: Schematic representation of the material electrical charge as a result of mechanical stress (Ruiz et al., 2007).

The relationship between the electrical charge generation and the mechanical stimuli is called the piezoelectric charge constant (*d*) and "represents the polarization charge generated per unit of mechanical stress (Soin et al., 2016)". The piezoelectric effect results from the orientation of the electrical dipoles in the molecule. Thus, the piezoelectric charge constant depends on the direction of the electrical charge produced by the piezoelectric and the direction of the applied mechanical stress/strain; those two directions must be indicated in the piezoelectric charge constant in tensorial form, as shown by Eq. 1, 2 (Moulson & Herbert, 2003; Uchino, 2018).

$$S_i = S_{ij}^E T_j + d_{ki} E_k \qquad (1)$$
$$D_i = d_{ij} T_j + \varepsilon_{ki}^T E_k \qquad (2)$$

S is the deformation, S^E is the elastic deformation under a constant electric field, *T* is the stress, *d* is the piezoelectric constant, and *E* is the electrical field tensor (Uchino, 2018). Piezoelectric materials have been used to extract energy from the ambient wind, sea waves, and vibration (Y. Wang, Yang, et al., 2020); the latter has attracted many researchers due to the facility to find mechanical vibration sources, making piezoelectric energy harvesting an exciting research topic.

Harvesting energy from the environment using piezoelectric devices is a viable option for backup energy to low-powered electronic devices. The energy quantity a piezoelectric device can produce is affected by the material piezoelectric properties, the mechanical configuration, the environmental conditions, and the electronics used to collect, store, and manage energy (Sodano et al., 2004).

The piezoelectric's equivalent electrical circuit is formed by an RCL series circuit in parallel with a capacitance, as shown in Figure 4 (Jaffe, 1958). This circuit presents two resonant conditions. One occurs when reactances on the RCL branch cancel each other, leading to low impedance (resonance frequency), and the second is when the RCL reactance equals the C_0 reactance, this condition is named antiresonance frequency (f_m, f_n respectively). Thus, the excitation frequency is a crucial parameter to be considered when designing a harvesting system based on piezoelectrics. It should be noted that this approach is valid when the ceramic is freely vibrating; under experimental conditions, the piezoelectric should be

modeled as a damped harmonic oscillator considering the harvesting system's physical restrictions.
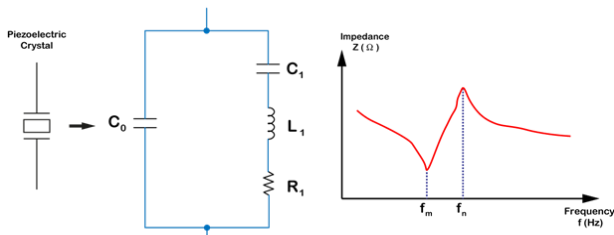
Figure 4: Equivalent electrical circuit of a piezoelectric and frequency-impedance spectrum.

The mechanical-to-electrical energy conversion at the resonance frequency has the highest value, even though the resonance frequency is usually higher than the vibration source. The piezoelectric element works at different frequencies for most of the vibrating conditions. Based on excitation frequency, two modes can be displayed in piezoelectric-based systems: in-resonance and off-resonance. Figure 5 shows standard configurations used to harvest energy using piezoelectrics, and each mode presents two different designs.
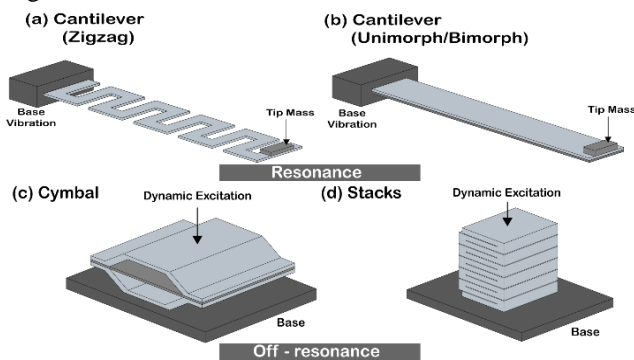
Figure 5: Common piezoelectric configurations for energy harvesting, (a), (b) resonance mode configurations, (c), (d) off-resonance configurations.

Three energy transfer mechanisms should be considered when setting up a piezoelectric energy harvesting application: mechanical to mechanical, mechanical to electrical, and electrical to electrical (Uchino, 2021). The mechanical-to-mechanical mechanism is called mechanical impedance and measures the energy transference from the mechanical source to the piezoelectric device. The mechanical-to-electrical transduction is related to the piezoelectric coefficients (d, g). Finally, the electrical-to-electrical transfer refers to the electrical impedance between the piezo element and the forward electronics.

1.2. Triboelectric generators

Triboelectrification (TE) has been known as an example of electrical charge generation for centuries. The Van de Graaff generator is an example of this type of device. Triboelectric generators (TENG) are based on electrostatic induction and contact electrification. Triboelectrification is defined as electric charge generation on a material surface resulting from the physical contact between two materials (Dagdeviren et al., 2017; Li et al., 2021; G. Zhu et al., 2012). When two materials come in contact, an electrical-charge results at the contact surfaces; due to a potential barrier at the material surface, the charges remain at the material surface without dissipation for a variable time (Xu et al., 2018). Triboelectrification has been explained using different models. Wang and Wang (Z. L. Wang & Wang, 2019) describe the TE due to the electron transfer mechanism when the interatomic distance is shorter than usual. The thermionic emission is also proposed to model contact electrification (Xu et al., 2018).

The separation of those previously joined materials leaves extra charge on the materials producing the triboelectric charge; when those materials are not good electrical conductors, the produced electrical charges remain for a long time on the surfaces of the materials (Boag, 1953; Furfari, 2005). Electrical charges remain more prolonged at low temperatures than at high temperatures; thus, triboelectrification highly depends on temperature (Xu et al., 2018).

Because the electrical charge is confined at the surface of the contact materials when they are in contact, the charge is named short circuit transfer charge (Qsc), and the electric potential difference is zero. When the materials are separated, the accumulated charge turns into a net electric potential difference named the open-circuit voltage (Voc). The surface charge density can describe the capability to develop and accumulate electrical charges of specific materials.

Depending on the polarity of the developed charge resulting from triboelectrification, materials are divided into positive (lose electrons) and negative (gain electrons) (Z. L. Wang, 2013). Therefore, TENGs are enhanced using positive and negative pairs of materials; Table 1 shows some selected materials' triboelectric charge density (TECD) (Zou et al., 2019).

Triboelectric results from physical contact between two materials; therefore, four triboelectric generation modes can be considered as the fundamental modes of contact separation, lateral sliding, single electrode, and freestanding, presented in Figure 6 (Niu et al., 2014; S. Wang et al., 2013, 2014; Zhou et al., 2020; G. Zhu et al., 2012). The contact-separation mode (Figure 6a) consists of a top and a back electrode, the latter in contact with a dielectric. These electrodes move vertically, and the charge is developed during contact or separation. The lateral-sliding mode (Figure 6b) has a similar configuration to the contact separation mode. The difference is that the charge is developed when there is a relative displacement of the top electrode over the back one. In the single-electrode mode, the back electrode is electrically grounded, serving as a reference electrode, and the top electrode moves freely (Figure 6c). It is worth mentioning that this configuration is preferred to quantify the triboelectric properties of a specific material. The freestanding mode consists of two symmetrical electrodes and a dielectric layer that produces an asymmetric potential (Figure 6d).

The electric potential developed due to triboelectrification depends on the triboelectric generation mode. The electric potential's mathematical description must include the electrostatic induction and contact charging expressions (Zhou et al., 2020), electrical charge density, relative electrode displacement, vacuum permittivity, and other variables affecting the developed electric potential.
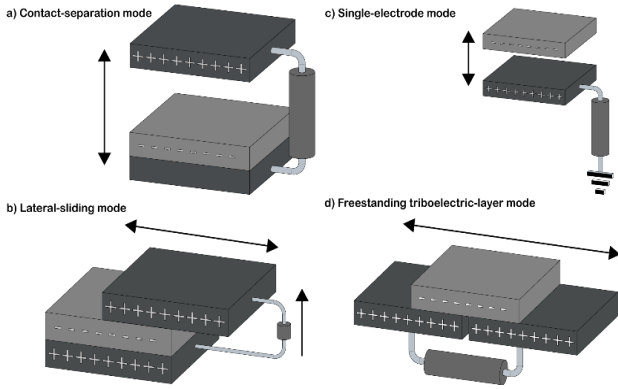
Figure 6: Main triboelectric generation modes for TENG development a) vertical contact separation, b) sliding, c) single-electrode, and d) freestanding triboelectric layer.

Table 1: Triboelectric charge density of selected triboelectric materials (adapted from (Zou et al., 2019) under CC license)

Material	Abbr.	Average TECD ($\mu C\ m^{-2}$)	STDEV (δ)
Clear Polyvinyl Chloride	PVC	-117.53	1.31
Polytetrafluoroethylene	PTFE	-113.06	1.14
Acrylonitrile Butadiene Styrene	ABS	-108.07	0.50
Clear Polycarbonate (Glossy)	PC	-104.63	1.79
Polystyrene	PS	-103.48	2.48
Ultem Polyetherimide	PEI	-102.91	2.16
Polydimethylsiloxane*	PDMS	-102.05	2.16
Polyimide Film	Kapton	-92.88	2.58
DuraLar Polyester Film	PET	-89.44	0.86
Polyvinylidene Fluoride	PVDF	-87.35	2.06
Polyetheretherketone	PEEK	-76.25	1.99
Polyethylene	PE	-71.20	1.71
Low-Density Polyethylene	LDPE	-67.94	1.49
High-Density Polyethylene	HDPE	-59.91	1.79
Clear Cast Acrylic	PMMA	-48.73	1.31
Poly(phenylene Sulfide)	PPS	-31.82	0.86
Polypropylene	PP	-27.23	1.31

1.3. *Thermoelectric generators*

Thermoelectric is the voltage generated in a material with opposite ends at different temperatures, as described in the Seebeck coefficient (Goldsmid,1964). When an electrically isolated material has a temperature difference (ΔT) between ends, a voltage difference can be measured, providing that no current flows between ends (Goldsmid, 1964; Li et al., 2021; Mahan, 2016), as Eq. 3 shows. Figure 7 shows a scheme of the classical thermoelectric configuration.

$$S(T_0) = \frac{\Delta V}{\Delta T} \tag{3}$$

where S is the Seebeck coefficient, an intrinsic property of each material, and T_0 is the temperature at which the coefficient is reported- because this property is temperature-dependent (Mahan, 2016).

Good electrical conductors have small Seebeck coefficient values, while bad conductors have high ones (Hofmann et al., 2019). Thermoelectric energy harvesters exploit a net temperature difference between two points [7]. Table 2 shows the Seebeck coefficients for the most common semiconductors used in thermoelectric generators.

Table 2: Seebeck coefficient for selected materials

Material	Abbr.	Seebeck coefficient S ($\mu V/K$)	Ref
Lead tellurium + Bismuth	PbTe Bi-doped	-284	(Harman et al., 2005)
Lead tellurium + Sodium	PbTe Na-doped	+254	(Harman et al., 2005)
	Se	+900	(Guan & Ouyang, 2021)
	Te	+500	(Guan & Ouyang, 2021)
	Sb_2Te_3	+185	(Guan & Ouyang, 2021)
	$Pb_3Ge_{39}Se_{58}$	+1670	(Guan & Ouyang, 2021)
	$Pb_{15}Ge_{37}Se_{58}$	-1990	(Guan & Ouyang, 2021)
	Bi_2Te_3	+230	(Guan & Ouyang, 2021)
	PEDOT:Tos	+30	(Guan & Ouyang, 2021)
	PPy	+10	(Guan & Ouyang, 2021)
	Poly(Ni-ett)	-125	(Guan & Ouyang, 2021)

In practice, the temperature difference between the device ends dependens on the device surfaces' thermal resistance, Figure 7; therefore, ΔT is lower than the net temperature difference between both sides of the device (Dagdeviren et al., 2017). The figure of merit (ZT) is presented in Eq. 4, which is the most used parameter for studying energy conversion efficiency; this formula relates the Seebeck coefficient (S), electrical conductivity (s), temperature (T), and thermal conductivity (κ) (Da Rosa & Ordóñez, 2021; Goldsmid, 1964).

$$ZT = T\left(\frac{S^2\sigma}{\kappa}\right) \tag{4}$$
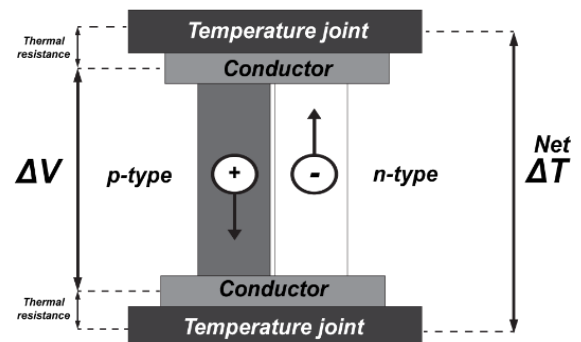
Figure 7: Thermoelectric scheme, the temperature difference is affected by the device's thermal resistance lowering the obtained energy.

1.4. *Electromagnetic generators*

The electromagnetic generators are based on Faraday's induction principle. The principle explains that any coil with a relative movement to a magnetic field will be induced with an electromagnetic field. Electromagnetic generators have two main parts, a coil, and a magnet, with relative movement between them. Based on the basic configuration, two arranges are used, fixed magnet, moving coil, and fixed coil moving magnet, as shown in Figure 8. Electromagnetic generators use different strategies to increase the output power, increasing the number of magnets and spires in the coil, using magnets with a higher magnetic field.
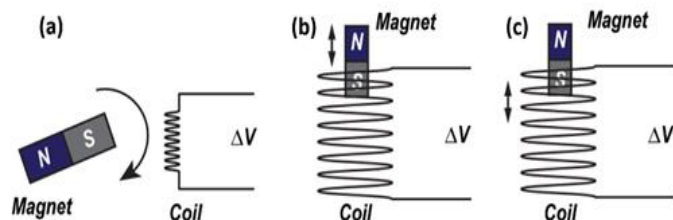
Figure 8: a) Externally induced coil. b) Induced coil with a moving magnet. c) Induction with a static magnet and moving coil.

Electromagnetic generators are of everyday use in high-power applications, but low-power applications arose with the development of stronger and smaller magnets.

2. Applications

2.1. *Piezoelectric*

Shehata and coworkers presented a poly (vinylidene fluoride) (PVDF) based membrane used for obtaining energy from acoustic signals (Shehata et al., 2020). The developed membrane was obtained by electrospun technique, and it was tested using a speaker excited with input voltages between 0.6 to 6 V and frequencies in the 100 Hz to 10kHz range. Shehata's results showed an output voltage of 350 mV when a 6 V signal was applied to the excitation source at a 4 kHz frequency.

2.2. *MEMS low resonance harvester*

A low-frequency resonant piezoelectric was developed by Song and colleagues (Song et al., 2017). This harvesting system is based on a spiral-shaped micromechanical system (MEMS). The spiral-shaped MEMS harvester was fabricated using a silicon wafer as substrate and PZT as active piezoelectric, designed for working at frequencies lower than 200 Hz. The operating frequency is crucial in the piezoelectric-based system because the piezoelectric response is frequency-dependent; most energy is lost when energy harvesters work in an off-resonance regime (Jaffe, 1958). Operating at the natural spiral frequency of 68 Hz, a power output of 23 nW with an active volume of 0.11 mm2, the resonance frequency can be tuned by modifying the spiral turns, and operating frequencies from 50 to 225 Hz can be achieved.

Hussein and Sabry present a composite structure in low-scale power generation devices (Sabry & Hussein, 2019). The proposed composite uses zinc oxide (ZnO), barium titanate (BaTiO3), and PVDF, all well-known piezoelectric materials. In the composite structure, ZnO nanorods and BaTiO3

nanospheres are dispersed homogeneously in dissolved PVDF; finally, the electrospun technique obtains composite fibers. The obtained composite can generate output voltages up to 12 V when low forces and frequencies are used, 1.5 N and 3.3 Hz, respectively (Sabry & Hussein, 2019).

A different approach to the structure of piezoelectric devices intended for energy harvesting is Han and co-authors' proposal (Han et al., 2019). 3D models in which wires and piezoelectric material are unified into a single complex microstructure are proposed instead of conventional single 2D or "flat" piezoelectric films.

3D microstructure microfabrication techniques were used to make this type of material. These microstructures are intended to resemble the shape of thin-film circuits frequently used in various electronics fields and devices. The microsystem layers consist of two electrodes, a layer for thickness, and a polyvinylidene difluoride (PVDF) layer as a piezoelectric material.

These microsystems are distributed in such a way as to form more complex 3D structures that contribute to the highest possible vibration collection, resulting in higher energy harvesting. A device such as a Figure 5a shows, whose structure is a 3D serpentine, can generate voltages above 1mV at 600 Hz to 700 Hz. This serpentine structure represents an improvement over conventional energy harvesters in that it can receive vibration from multiple directions, unlike cantilever-type arrangements that are bidirectional.

Another novelty studied in this manuscript is implementing this type of microstructure in three-dimensional biological systems; this was performed in the leg of a rodent, an area of the body representing a more significant amount of movement. An encapsulated 3D device was implanted to avoid contact with the fluids where it was placed. As the rodent moved, energy generation of about 100 µV began to be recorded. The rodent was placed in an enclosed area of 23 cm × 16 cm × 16 cm to monitor its movements. Its activity generated energy with peak voltages more significant than one mV. Such innovations to conventional energy harvesting systems open the way for further research in potential application areas such as robotics and biomedical implants.

2.3. *Triboelectric*

Energy generation sources that occur due to friction, apart from traditional configurations, new approaches are arising; based on origami, a TENG device is presented by Wang and coworkers (Y. Wang, Wu, et al., 2020); this device is built with a double helix shape and distributed in a folded paper. A scheme of the mentioned device is presented in Figure 9. A polytetrafluoroethylene (PTFE) film serves as an electrical generator. The working principle of this device is the electrical charge transference between two materials (copper and PTFE) with a significant electronegativity difference. Copper foil works as the electrode and induces potential differences by folding and unfolding the electrical device (Fig. 9). A downward charge transfer occurs between the copper foil and PTFE when the device moves upward. Electrical power up to 580 µW on a 20 MΩ load can be reached. As a drawback, the device needs a protective coating when used in outdoor applications since exposed copper and its corrosion would present disadvantages in the correct energy generation.
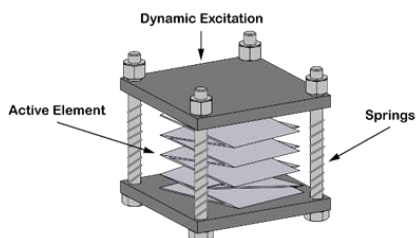
Figure 9: 3D schematic of the basic unit of an origami-based triboelectric generator device (Y. Wang, Wu, et al., 2020)

Another triboelectric generator is presented by Wang and collaborators (Y. Wang, Yang, et al., 2020); this approach was inspired by flag behavior. It represents an approximation to 2D design, which means the flag-type nanogenerator uses futtering induced by wind and rain.

Carbon-coated polyethylene terephthalate membranes and polytetrafluoroethylene are the active elements composing this device. The energy output strongly depends on flag dimensions and wind speed. With flag dimensions of 150×75 mm and wind speed of 7.5 m / s, the generated current is 6.8 µA, and a peak power of 36.72 µW can be reached over a 5 MΩ as load resistance- additionally, the device has the capability for measuring wind velocity and direction.

A dripping-based nanogenerator is a novel approach to energy generation resulting from the triboelectric phenomenon. This system is focused on transferring liquid from one container to another by dripping (Y. Wang, Wu, et al., 2020). Zhong and collaborators describe the construction of a dripping channel based on L-TENG (Zhong et al., 2020) that collects energy using electrification from liquid to solid due to electron transfer. Parallel to this, it detects the dripping frequency and the number of droplets that contact the channel. This device comprises two flat panels distributed as a two slopes structure (Figure 10). Each panel comprises a PTFE film, a layer composed of gold and copper materials, and a final layer of epoxy glass fiber which gives rigid support to the previous layers. The copper and gold layers are distributed in a grating-electrode structure electrode, which will be the device's energy harvester. This L-TENG has a single electrode used for sensing functions like identifying the number of droplets, the time interval between drops, and the total duration of the droplets.
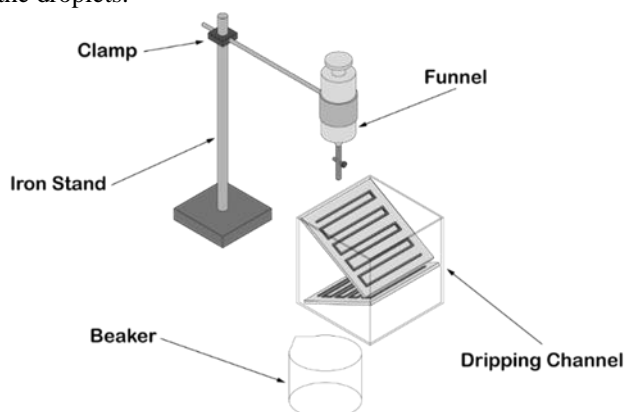
Figure 10: Dripping channel system design (Zhong et al., 2020).

The slope arrangement provides a maximum output power compared with a single ramp or unfolded structure. Three tests were carried out with 0.2, 0.4, and 0.6 m panels and the results indicate that the best performance is obtained with the 0.4 m panel, whose charge and voltage levels were higher than the others, reaching 484.98 nW with a 40.7 MΩ load. According to Equation 5, the energy generated by a single drop in each of the three cases was calculated. The results were 12.76 nJ, 141.41 nJ, and 93.99 nJ for 0.2 m, 0.4 m, and 0.6 m, respectively.

$$E = \frac{\int_0^{T_E} I^2 R \, dt}{20} \tag{5}$$

It has the disadvantage that, as it is a chemical process, there is a risk of contaminating the droplets by subjecting them to contact with a "third element" (the harvesting panels). However, this process could help in raindrop energy harvesting applications, where even a piezoelectric collection device can be added. This type of device can be advantageous in intelligent systems in laboratories where a census and control of data are required and can take advantage of specific procedures for energy harvesting purposes.

2.4. Thermoelectric

Recent studies have attempted to study thermoelectric devices' energy harvesting and power generation capabilities with the rise of wearable electronics technology. Lund and coworkers use a conductive polymer to develop a thermoelectric textile (Lund et al., 2020). The proposed thermoelectric textile uses the temperature difference between the body and the surrounding environment. Textile provides up to 8mV when the temperature difference is 65 K with a peak power of 1.2 µW. The textile's electrical behaviour can be modeled using standard thermoelectric models when thermal and electrical resistance are included.

A flexible thermoelectric device is proposed by Lu and collaborators (Lu et al., 2014). This thermoelectric device is fabricated using the direct inkjet printing technique. It uses p-type and n-type nanoparticles (Fig. 11). This device's maximum thermopower is 341µV/K at 50 °C for the most straightforward configuration. It is worth commenting that the inkjet printing technique is easy to handle, but low density and low electrical conductivity are achieved when using this technique.

Wang and coworkers studied a self-powered and self-moving device. They propose energy generation through a Thermo-Mechano-Electrical-System (TMES) (X.-Q. Wang et al., 2018). The device consists of converting this harvested energy into mechanical movements. Movements generate electrical energy because the structure of the device is composed of layers of materials such as PVDF (ferroelectric polyvinylidene fluoride) and PDG-CNT (polydopamine modified, reduced graphene oxide-carbon nanotube).

The thermo-mechanical feedback process involves the system's activation through temperature as the first stage. When the TMES is placed on a hot surface, deformation begins at the PDG-CNT layer. The temperature causes a deformation, which provokes a piezoelectric effect at the PVDF layer, as Figure 11 shows. Deformation caused by the temperature can

occur even when the temperature is 27.2 °C. The TMES reaches a steady state at 55-65 °C, meaning it will be in a 2D repeated self-locomotion in this temperature range. The energy generated from the material's deformation results in voltage peaks from 24 V to 67 V. In the proposed configuration, higher temperatures lead to higher material deformation and pronounced energy peaks.
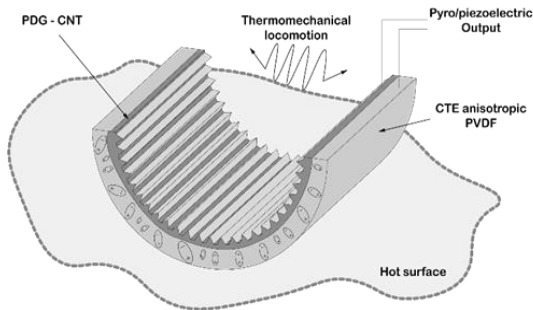
Figure 11: Thermo-Mechano-Electrical-System (X.-Q. Wang et al., 2018).

Solar energy has been a studied phenomenon for electric power generation for a long time. This manuscript studies a device that takes advantage of one of the characteristics of solar energy, temperature. This device studies the ability to harvest thermoelectric energy based on solar radiations using a commercial thermoelectric module based on Al_2O_3.

This module was coated with candle flame soot to analyze the effects of having this soot layer between the solar rays and the thermoelectric module.

As part of the energy harvesting/management system, a DC-DC boost converter was added, whose design is composed of a Schottky diode, a 30 mH inductor, and a MOSFET.

Several tests were performed with the module with and without the soot coating at different temperatures with a load resistance of 50 ohms. These tests showed that the best performance was obtained with the soot-coated module reaching a value of 10 mW. This type of system is considered ideal for powering low-power electronics.

2.5. Electromagnetic conversion applications

The transformation of motion phenomena can be considered the primary means of energy harvesting. Naifar and collaborators (Naifar et al., 2020) propose an electromagnetic transducer; this device relies on electromagnetic induction by implementing a second-order linear oscillator for harvesting energy in vibrating environments. The proposed device uses a mass-spring-damping system implemented on a moving coil mechanically coupled to fixed magnets and a mechanical spring; hence the vibration changes into an axial movement displacing the coil through the magnet; hence electromagnetic charges have induced the coil.

The output voltage rises 5V with frequencies between 10 and 100 Hz, but the proposed device can work with frequencies up to 500 Hz; 68 µJ can be reached in resonant conditions.

The management and control of the direction of movement can be translated into power generation, as demonstrated by Luo and collaborators (Luo et al., 2020). They present a linear to rotary movement converter device. The linear movement is changed into rotary movement by using a twist-driving system. The rotary energy harvester is complemented by placing magnets in the external circumference of the rotator part of this system and coils in the internal circumference of the stator. The linear movement makes the rotor turn, and electromagnetic charges are induced into coils. Fig. 12 shows the catch-driving process. One of the critical features of this system is the possibility of working at ultralow frequencies even lower than 1 Hz. Output power up to 4.5 mW at 0.84 Hz can be achieved on an 85 Ω load.
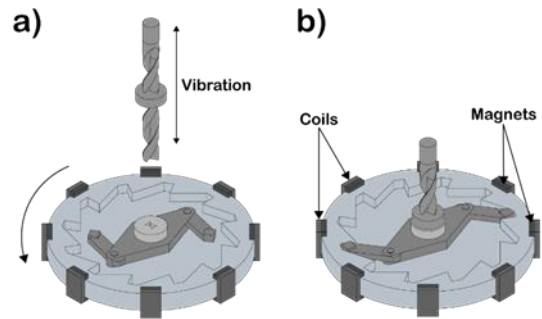
Figure 12: a) Linear to rotate movement conversion, b) velocity conversion, c) fixation mechanism for maintaining the rotation in a unique direction, d) electromagnetic transduction detail (Luo et al., 2020).

A cup-shaped electromagnetic generator designed to harvest energy from the human body is presented by Yuham and coworkers (Gu et al., 2020). The generator is a cup-shaped device; six coils are distributed in its periphery; inside, a trajectory is built to allow the magnetic ball's movement. The magnetic ball induces an electromagnetic charge when passing close to coils. This magnetic ball is made of neodymium iron boron (NdFeB), and its function is to oscillate according to the movement of the human body. In this case, different tests were performed by placing the device on different parts of the body, such as the wrist, ankle, knee, and arm, and on a backpack placed on the test subject's back in order to deduce where the most significant oscillation occurred, which translates into greater energy generation. The tests were performed with a person walking on a treadmill- with eight load resistance values between 5Ω and 100Ω, being 30Ω the optimal value. The harvested energy is calculated according to Equation 6.

$$P = \frac{1}{T}\int_t^{t+T} I_{eq}^2 R_L dt = \frac{1}{2}I_{rms}^2 R_L \qquad (6)$$

Where:

R_L Load resistance (Ω), I_{rms} Root Mean Square current value, I_{eq} Equivalent current, P Harvested Power, T time for calculation, t Initial time, respectively.

This experiment was performed with a test subject moving on a treadmill at speeds from 2 km/h to 14 km/h (Luo et al., 2020). It is possible to deduce that the more movement the body has, the more energy will be generated. However, this is not optimal since more movement involves more effort. By placing the device on the test subject's ankle and moving at 5 km/h, there is an optimal generation, reaching 1.4 mW. This device can be annoying due to its size and the magnetic ball that shakes with any movement.

Another configuration used to harvest energy is the one used by Rosales and Gonzalez (Rosales & Landaeta, 2021), in which a walk-aid device is used to get energy. In the proposed device,

three coils and a pendulous magnet is placed in a gait support for the elderly. Coils positions were determined to use the full travel in a pendulum-free movement. The system was designed to consider the total weight not to affect the walker's weight significantly. The maximum voltage was 2.2 volts.

2.6. Overview of the analyzed devices

Table 3: shows the power output comparative among the described devices. Harvested power ranges from nano to mV in all the studied cases.

Table 3: Power output comparison among studied methods.

Physical mechanism		Operating frequencies	Power output	Ref.
Piezo electric	Acoustic harvester	<10 kHz	100 nW	(Shehata et al., 2020)
	Resonance harvester	<200 Hz	23 nW	(Song et al., 2017)
	Composite nanogenerator	3.3 Hz	12 V	(Sabry & Hussein, 2019)
	Vibrational	<700 Hz	1 mV	(Han et al., 2019)
Tribo electric	Origami-based	6 Hz	580 µW	(Y. Wang, Wu, et al., 2020)
	Flag-type	N/A	36.72 µW	(Y. Wang, Yang, et al., 2020)
	Dripping	N/A	484.98 nW	(Zhong et al., 2020)
Thermo electric	Textile	N/A	1.2 µW	(Lund et al., 2020)
	Thermo-mechanical	N/A	24 V	(X.-Q. Wang et al., 2018)
Electro magnetic	Linear oscillator	500 Hz	68 µJ	(Naifar et al., 2020)
	Inertial rotary	0.84 Hz	4.5 mW	(Luo et al., 2020)
	Cup-shaped	8 Hz	1.4 mW	(Gu et al., 2020)
	Mass damper	1 Hz	50.6 W	(H. Zhu et al., 2019)

3. Conclusions

Different energy harvesting configurations have limitations: Piezoelectric-based systems have small power generation compared with semiconductors, time-dependent signals, low operation current, high-temperature dependence, and strongly dependent poling direction in crystals and fragility of the ceramics. In polymers, low-temperature operation range. The triboelectric-based generators are limited by the slow charge accumulation and inherent charge leakage, lowering the charge density. When electrical isolation and better charge capabilities are achieved, triboelectric-based systems can be chosen for low-power applications ranging from health to mobile devices. Thermoelectric devices are limited by the device's thermal resistance and strongly depend on a temperature difference.

However, even though the amount of energy generated is not very large, this device allows us to obtain energy from almost any physical phenomenon. The advance of low and ultralow-power electronics makes energy harvesting the right path for developing self-powered devices. Energy harvesting

represents an advantage since the energy generated can be managed more efficiently and, besides, it can be increased to the desired quantities (in reasonable ranges concerning generation) with the proper electronics arrangements.

Each configuration has its development way, but there are two main paths for energy harvesting, low power for building self-powered devices, as in biomedical devices, and high-power applications as a backup for commercial applications. The obtained power should be enough to guarantee the function of the target device; in addition, the power must be high enough to serve as an actual energy harvester and not only as a sensor.

Referencias

Al-Nabulsi, J., El-Sharo, S., Salawy, N., & Al-Doori, H. (2019). Methods of energy generation from the human body: A literature review. *Journal of Medical Engineering & Technology*, *43*(4), 255–272. https://doi.org/10.1080/03091902.2019.1658818

Boag, J. W. (1953). The design of the electric field in a Van de Graaff generator. *Proceedings of the IEE-Part IV: Institution Monographs*, *100*(5), 63–82.

Da Rosa, A. V., & Ordóñez, J. C. (2021). *Fundamentals of renewable energy processes*. Academic Press.

Dagdeviren, C., Li, Z., & Wang, Z. L. (2017). Energy Harvesting from the Animal/Human Body for Self-Powered Electronics. *Annual Review of Biomedical Engineering*, *19*(1), 85–108. https://doi.org/10.1146/annurev-bioeng-071516-044517

Furfari, F. A. (2005). A history of the Van de Graaff generator. *IEEE Industry Applications Magazine*, *11*(1), 10–14.

Goldsmid, H. J. (1964). Transport processes in metals and semiconductors. In *Thermoelectric Refrigeration* (pp. 12–41). Springer.

Gu, Y., Liu, W., Zhao, C., & Wang, P. (2020). A goblet-like non-linear electromagnetic generator for planar multi-directional vibration energy harvesting. *Applied Energy*, *266*, 114846.

Guan, X., & Ouyang, J. (2021). Enhancement of the Seebeck coefficient of organic thermoelectric materials via energy filtering of charge carriers. *CCS Chemistry*, *3*(10), 2415–2427.

Han, M., Wang, H., Yang, Y., Liang, C., Bai, W., Yan, Z., Li, H., Xue, Y., Wang, X., & Akar, B. (2019). Three-dimensional piezoelectric polymer microsystems for vibrational energy harvesting, robotic interfaces and biomedical implants. *Nature Electronics*, *2*(1), 26–35.

Harman, T. C., Walsh, M. P., Laforge, B. E., & Turner, G. W. (2005). Nanostructured thermoelectric materials. *Journal of Electronic Materials*, *34*, L19–L22.

Hofmann, A. I., Kroon, R., & Müller, C. (2019). Doping and processing of organic semiconductors for plastic thermoelectrics. In *Handbook of Organic Materials for Electronic and Photonic Devices* (pp. 429–449). Elsevier.

Jaffe, H. (1958). Piezoelectric Ceramics. *Journal of the American Ceramic Society*, *41*(11), 494–498. https://doi.org/10.1111/j.1151-2916.1958.tb12903.x

Jonathan Adams. (2019, April 26). *A Collaborative Approach to Enhancing Research Discovery*. Dimensions. https://www.dimensions.ai/resources/a-collaborative-approach-to-enhancing-research-discovery/

Li, Y., Zhao, Z., Liu, L., Zhou, L., Liu, D., Li, S., Chen, S., Dai, Y., Wang, J., & Wang, Z. L. (2021). Improved output performance of triboelectric nanogenerator by fast accumulation process of surface charges. *Advanced Energy Materials*, *11*(14), 2100050.

Lu, Z., Layani, M., Zhao, X., Tan, L. P., Sun, T., Fan, S., Yan, Q., Magdassi, S., & Hng, H. H. (2014). Fabrication of flexible thermoelectric thin film devices by inkjet printing. *Small (Weinheim an Der Bergstrasse, Germany)*, *10*(17), 3551–3554. https://doi.org/10.1002/smll.201303126

Lund, A., Tian, Y., Darabi, S., & Müller, C. (2020). A polymer-based textile thermoelectric generator for wearable energy harvesting. *Journal of Power Sources*, *480*, 228836. https://doi.org/10.1016/j.jpowsour.2020.228836

Luo, A., Zhang, Y., Dai, X., Wang, Y., Xu, W., Lu, Y., Wang, M., Fan, K., & Wang, F. (2020). An inertial rotary energy harvester for vibrations at ultra-low frequency with high energy conversion efficiency. *Applied Energy*, *279*, 115762.

Mahan, G. D. (2016). Thermoelectric Effect. In *Reference Module in Materials Science and Materials Engineering*. Elsevier. https://doi.org/10.1016/B978-0-12-803581-8.01291-1

Moulson, A. J., & Herbert, J. M. (2003). *Electroceramics: Materials, Properties, Applications*. John Wiley & Sons.

Naifar, S., Trigona, C., Bradai, S., Baglio, S., & Kanoun, O. (2020). Characterization of a smart transducer for axial force measurements in vibrating environments. *Measurement*, *166*, 108157. https://doi.org/10.1016/j.measurement.2020.108157

Niu, S., Liu, Y., Wang, S., Lin, L., Zhou, Y. S., Hu, Y., & Wang, Z. L. (2014). Theoretical investigation and structural optimization of single-electrode triboelectric nanogenerators. *Advanced Functional Materials*, *24*(22), 3332–3340.

Rosales, V. R., & Landaeta, R. E. G. (2021). Propuesta de un péndulo electromagnético para la recolección de energía en usuarios de dispositivos de soporte de la marcha. *Memorias Del Congreso Nacional de Ingeniería Biomédica*, *8*(1), 138–141.

Ruiz, R. R., Cuautle, A. F., & Gomez, E. S. (2007). Development of lead-free (Bi1/2Na1/2) BaTiO3 Piezoelectric Ceramics for Clinical Applications in Ultrasound. *2007 4th International Conference on Electrical and Electronics Engineering*, 75–78. https://doi.org/10.1109/ICEEE.2007.4344977

Sabry, R. S., & Hussein, A. D. (2019). PVDF: ZnO/BaTiO3 as high out-put piezoelectric nanogenerator. *Polymer Testing*, *79*, 106001.

Shehata, N., Hassanin, A. H., Elnabawy, E., Nair, R., Bhat, S. A., & Kandas, I. (2020). Acoustic energy harvesting and sensing via electrospun PVDF nanofiber membrane. *Sensors*, *20*(11), 3111.

Sodano, H. A., Inman, D. J., & Park, G. (2004). A Review of Power Harvesting from Vibration Using Piezoelectric Materials. *The Shock and Vibration Digest*, *36*(3), 197.

Soin, N., Anand, S. C., & Shah, T. H. (2016). 12—Energy harvesting and storage textiles. In A. R. Horrocks & S. C. Anand (Eds.), *Handbook of Technical Textiles (Second Edition)* (pp. 357–396). Woodhead Publishing. https://doi.org/10.1016/B978-1-78242-465-9.00012-4

Song, H.-C., Kumar, P., Maurya, D., Kang, M.-G., Reynolds, W. T., Jeong, D.-Y., Kang, C.-Y., & Priya, S. (2017). Ultra-low resonant piezoelectric MEMS energy harvester with high power density. *Journal of Microelectromechanical Systems*, *26*(6), 1226–1234.

Thelwall, M. (2018). Dimensions: A competitor to Scopus and the Web of Science? *Journal of Informetrics*, *12*(2), 430–435. https://doi.org/10.1016/j.joi.2018.03.006

Uchino, K. (2018). *Ferroelectric Devices*. CRC Press.

Uchino, K. (2021). Misconceptions in Piezoelectric Energy-Harvesting System Development. *Engineering Proceedings*, *4*(1), Article 1. https://doi.org/10.3390/Micromachines2021-09570

van Eck, N. J., & Waltman, L. (2010). Software survey: VOSviewer, a computer program for bibliometric mapping. *Scientometrics*, *84*(2), 523–538. https://doi.org/10.1007/s11192-009-0146-3

Wang, S., Lin, L., Xie, Y., Jing, Q., Niu, S., & Wang, Z. L. (2013). Sliding-triboelectric nanogenerators based on in-plane charge-separation mechanism. *Nano Letters*, *13*(5), 2226–2233.

Wang, S., Xie, Y., Niu, S., Lin, L., & Wang, Z. L. (2014). Freestanding triboelectric-layer-based nanogenerators for harvesting energy from a moving object or human motion in contact and non-contact modes. *Advanced Materials*, *26*(18), 2818–2824.

Wang, X.-Q., Tan, C. F., Chan, K. H., Lu, X., Zhu, L., Kim, S.-W., & Ho, G. W. (2018). In-built thermo-mechanical cooperative feedback mechanism for self-propelled multimodal locomotion and electricity generation. *Nature Communications*, *9*(1), 1–10.

Wang, Y., Wu, Y., Liu, Q., Wang, X., Cao, J., Cheng, G., Zhang, Z., Ding, J., & Li, K. (2020). Origami triboelectric nanogenerator with double-helical structure for environmental energy harvesting. *Energy*, *212*, 118462. https://doi.org/10.1016/j.energy.2020.118462

Wang, Y., Yang, E., Chen, T., Wang, J., Hu, Z., Mi, J., Pan, X., & Xu, M. (2020). A novel humidity resisting and wind direction adapting flag-type triboelectric nanogenerator for wind energy harvesting and speed sensing. *Nano Energy*, *78*, 105279. https://doi.org/10.1016/j.nanoen.2020.105279

Wang, Z. L. (2013). Triboelectric nanogenerators as new energy technology for self-powered systems and as active mechanical and chemical sensors. *ACS Nano*, *7*(11), 9533–9557.

Wang, Z. L., & Wang, A. C. (2019). On the origin of contact-electrification. *Materials Today*, *30*, 34–51.

Xu, C., Zi, Y., Wang, A. C., Zou, H., Dai, Y., He, X., Wang, P., Wang, Y.-C., Feng, P., & Li, D. (2018). On the electron-transfer mechanism in the contact-electrification effect. *Advanced Materials*, *30*(15), 1706790.

Zhong, W., Xu, L., Zhan, F., Wang, H., Wang, F., & Wang, Z. L. (2020). Dripping channel based liquid triboelectric nanogenerators for energy harvesting and sensing. *Acs Nano*, *14*(8), 10510–10517.

Zhou, L., Liu, D., Wang, J., & Wang, Z. L. (2020). Triboelectric nanogenerators: Fundamental physics and potential applications. *Friction*, *8*, 481–506.

Zhu, G., Pan, C., Guo, W., Chen, C.-Y., Zhou, Y., Yu, R., & Wang, Z. L. (2012). Triboelectric-generator-driven pulse electrodeposition for micropatterning. *Nano Letters*, *12*(9), 4960–4965.

Zhu, H., Li, Y., Shen, W., & Zhu, S. (2019). Mechanical and energy-harvesting model for electromagnetic inertial mass dampers. *Mechanical Systems and Signal Processing*, *120*, 203–220.

Zou, H., Zhang, Y., Guo, L., Wang, P., He, X., Dai, G., Zheng, H., Chen, C., Wang, A. C., & Xu, C. (2019). Quantifying the triboelectric series. *Nature Communications*, *10*(1), 1427.